

Measurement of electronic structure in van der Waals ferromagnet $Fe_{5-x}GeTe_2$

Kui Huang(黄逵), Zhenxian Li(李政贤), Deping Guo(郭的坪), Haifeng Yang(杨海峰), Yiwei Li(李一苇),Aiji Liang(梁爱基), Fan Wu(吴凡), Lixuan Xu(徐丽璇), Lexian Yang(杨乐仙), Wei Ji(季威),Yanfeng Guo(郭艳峰), Yulin Chen(陈宇林), and Zhongkai Liu(柳仲楷)

Citation: Chin. Phys. B, 2022, 31 (**5**): 057404. DOI: 10.1088/1674-1056/ac5c3c
Journal homepage: http://cpb.iphy.ac.cn; http://iopscience.iop.org/cpb

What follows is a list of articles you may be interested in

Surface-induced orbital-selective band reconstruction in kagome superconductor CsV_3Sb_5

Linwei Huai(淮琳崴), Yang Luo(罗洋), Samuel M. L. Teicher, Brenden R. Ortiz, Kaize Wang(王铠泽),Shuting Peng(彭舒婷), Zhiyuan Wei(魏志远), Jianchang Shen(沈建昌), Bingqian Wang(王冰倩), Yu Miao(缪宇),Xiupeng Sun(孙秀鹏), Zhipeng Ou(欧志鹏), Stephen D. Wilson, and Junfeng He(何俊峰)

Chin. Phys. B, 2022, 31 (**5**): 057403. DOI: 10.1088/1674-1056/ac4f50

Anomalous spectral weight transfer in the nematic state of iron-selenide superconductor

C Cai(蔡淙), T T Han(韩婷婷), Z G Wang(王政国), L Chen(陈磊), Y D Wang(王宇迪), Z M Xin(信子鸣), M W Ma(马明伟), Yuan Li(李源), Y Zhang(张焱)

Chin. Phys. B, 2020, 29 (**7**): 077401. DOI: 10.1088/1674-1056/ab90ec

Direct observation of the f-c hybridization in the ordered uranium films on W(110)

Qiuyun Chen(陈秋云), Shiyong Tan(谭世勇), Wei Feng(冯卫), Lizhu Luo(罗丽珠), Xiegang Zhu(朱燮刚), Xinchun Lai(赖新春)

Chin. Phys. B, 2019, 28 (**7**): 077404. DOI: 10.1088/1674-1056/28/7/077404

Electronic structure of heavy fermion system $CePt_2In_7$ from angle-resolved photoemission spectroscopy

Bing Shen(沈兵), Li Yu(俞理), Kai Liu(刘凯), Shou-Peng Lyu(吕守鹏), Xiao-Wen Jia(贾小文), E D Bauer, J D Thompson, Yan Zhang(张艳), Chen-Lu Wang(王晨露), Cheng Hu(胡成), Ying Ding(丁颖), Xuan Sun(孙璇), Yong Hu(胡勇), Jing Liu(刘静), Qiang Gao(高强), Lin Zhao(赵林), Guo-Dong Liu(刘国东), Zu-Yan Xu(许祖彦), Chuang-Tian Chen(陈创天), Zhong-Yi Lu(卢仲毅), X J Zhou(周兴江)

Chin. Phys. B, 2017, 26 (**7**): 077401. DOI: 10.1088/1674-1056/26/7/077401

Angle-resolved photoemission spectroscopy study on iron-based superconductors

Ye Zi-Rong, Zhang Yan, Xie Bin-Ping, Feng Dong-Lai

Chin. Phys. B, 2013, 22 (**8**): 087407. DOI: 10.1088/1674-1056/22/8/087407

RAPID COMMUNICATION

Measurement of electronic structure in van der Waals ferromagnet $Fe_{5-x}GeTe_2$

Kui Huang(黄逵)[1,2,3], Zhenxian Li(李政贤)[1], Deping Guo(郭的坪)[4], Haifeng Yang(杨海峰)[1], Yiwei Li(李一苇)[1,5], Aiji Liang(梁爱基)[1,5], Fan Wu(吴凡)[1], Lixuan Xu(徐丽璇)[6], Lexian Yang(杨乐仙)[6], Wei Ji(季威)[4], Yanfeng Guo(郭艳峰)[1], Yulin Chen(陈宇林)[1,5,7,†], and Zhongkai Liu(柳仲楷)[1,5,‡]

[1] *School of Physical Science and Technology, ShanghaiTech University, Shanghai* 200031, *China*
[2] *Shanghai Institute of Optics and Fine Mechanics, Chinese Academy of Sciences, Shanghai* 201800, *China*
[3] *University of Chinese Academy of Sciences, Beijing* 100049, *China*
[4] *Department of Physics and Beijing Key Laboratory of Opto-electronic Functional Materials & Micro-nano Devices, Renmin University of China, Beijing* 100190, *China*
[5] *ShanghaiTech Laboratory for Topological Physics, ShanghaiTech University, Shanghai* 201210, *China*
[6] *State Key Laboratory of Low Dimensional Quantum Physics and Department of Physics, Tsinghua University, Beijing* 100084, *China*
[7] *Department of Physics, University of Oxford, Oxford OX*1 3*PU, United Kingdom*

(Received 13 January 2022; revised manuscript received 3 March 2022; accepted manuscript online 10 March 2022)

As a van der Waals ferromagnet with high Curie temperature, $Fe_{5-x}GeTe_2$ has attracted tremendous interests recently. Here, using high-resolution angle-resolved photoemission spectroscopy (ARPES), we systematically investigated the electronic structure of $Fe_{5-x}GeTe_2$ crystals and its temperature evolution. Our ARPES measurement reveals two types of band structures from two different terminations with slight k_z evolution. Interestingly, across the ferromagnetic transition, we observed the merging of two split bands above the Curie temperature, suggesting the band splitting due to the exchange interaction within the itinerant Stoner model. Our results provide important insights into the electronic and magnetic properties of $Fe_{5-x}GeTe_2$ and the understanding of magnetism in a two-dimensional ferromagnetic system.

Keywords: angle-resolved photoemission spectroscopy, van der Waals ferromagnet, electronic structure

PACS: 74.25.Jb, 71.20.−b, 31.15.A−, 77.80.B− **DOI:** 10.1088/1674-1056/ac5c3c

1. Introduction

Recently, van der Waals (vdW) ferromagnets have attracted great research attention because they provide a versatile playground to explore the nature of the low-dimensional magnetism and a rich material basis for future applications: the vdW ferromagnets in the 2D limit exhibit unusual properties such as large magnetic anisotropy, (quantum) anomalous Hall effect, long-range magnon transport, etc.[1–6] Furthermore, their virtue of easy exfoliation into few-layer limit makes them very convenient for constructing various novel heterostructures and devices, which would find potential applications in the next-generation spintronic devices, such as spin valves, spin–orbit torque, spin field-effect transistors, spin tunneling field-effect transistors, and spin-filter magnetic tunnel junctions.

In principle, in the isotropic 2D limit, the spontaneous symmetry breaking for the formation of intrinsic long-range magnetic order is generally prohibited by strong thermal fluctuations, which is known as the Merin–Wagner theorem.[7] Nevertheless, the long-range magnetic order has been realized in a broad range of vdW ferromagnets, such as in mono- or few-layer CrI_3,[1] $Cr_2Ge_2Te_6$,[2] $Cr_2Si_2Te_6$,[8] VSe_2,[9] and $MnSe_2$,[10] etc., owing to their intrinsic magnetocrystalline anisotropy.

Among all the vdW ferromagnets, Fe_xGeTe_2 is an intriguing material class with large intrinsic anomalous Hall effect, high Curie temperature (T_c) and highly tunable magnetic properties with different chemical composition, layer thickness, and external gating.[11–15] As for Fe_3GeTe_2, while the transport and optical methods have revealed 2D itinerant ferromagnetism, previous angle resolved photoemission spectroscopy (ARPES) measurement has suggested signature for non-Stoner ferromagnetism,[13] therefore the origin of the magnetic ordering as well as its interplay with the electronic structure remains mysterious and requires further investigations.

To address the issue, the investigation of new member $Fe_{5-x}GeTe_2$ becomes critical.[16–22] $Fe_{5-x}GeTe_2$ shows the highest T_c (from 270 K to 363 K depending on the Fe deficiency x) among the Fe_xGeTe_2 family, since the extra Fe layer in $Fe_{5-x}GeTe_2$ can considerably enhance the magnetic interaction and stabilize the long-range magnetic order. However, limited by the much less study on $Fe_{5-x}GeTe_2$ as compared with Fe_3GeTe_2, the underlying mechanisms for the room tem-

†Corresponding author. E-mail: yulin.chen@physics.ox.ac.uk
‡Corresponding author. E-mail: liuzhk@shanghaitech.edu.cn
© 2022 Chinese Physical Society and IOP Publishing Ltd

perature T_c remain mysterious and the relation between the magnetic order and electronic structure in $Fe_{5-x}GeTe_2$ requires further investigations.

In this work, we systematically studied the electronic structure of $Fe_{5-x}GeTe_2$ using synchrotron-based ARPES and made the following discoveries. First, we have observed two kinds of band structures from two different cleaved terminations in $Fe_{5-x}GeTe_2$. Second, our photon energy dependence measurement shows clear periodicity of $2\pi/c$ in the electronic structure and slight variation in the band structure, which suggests the 2D nature of $Fe_{5-x}GeTe_2$. Finally, the temperature evolution of electronic structure of $Fe_{5-x}GeTe_2$ suggests the merging of two bands which are ~ 400 meV apart across the Curie temperature. We conclude that the exchange-splitting observed in the electronic structure indicates that the itinerant Stoner model properly describes the origin of ferromagnetism in $Fe_{5-x}GeTe_2$. Our observation provides important insights into the nature of ferromagnetism of $Fe_{5-x}GeTe_2$ and other two-dimensional ferromagnetic materials.

2. Result and discussion

High-quality $Fe_{5-x}GeTe_2$ single crystals were grown from chemical vapor transport technique by using iodine as the transport agent, similar as the method described in Refs. [17,23]. The crystal structure is the rhombohedral lattice with space group $R\bar{3}m$ (No. 166) (see Fig. 1(a) for the conventional cell). The $Fe_{5-x}GeTe_2$ unit cell is composed of two octuple layers bounded by the vdW force, each arranged as Te–Fe(1)–Fe(2)–Ge–Fe(3)–Fe(4)–Fe(5)–Te and Te–Fe(5)–Fe(4)–Fe(3)–Ge–Fe(2)–Fe(1)–Te, where Fe atoms occupy 5 different sublayers. Two kinds of terminations could be obtained after the cleavage along its (0001) direction with Fe(1) or Fe(5) as the top-most Fe layers (Fig. 1(a)). The corresponding Brillouin zone (BZ), its projection to the (0001) surface and the high-symmetry points are illustrated in Fig. 1(b). The samples typically appear in lamelliform as shown in Fig. 1(c), and the high quality could be verified by the x-ray diffraction (XRD) (Fig. 1(c)), from which the conventional lattice constants can be extracted as $a = b = 4.05$ Å, $c = 29.23$ Å. The ferromagnetism of the compound is characterized by the temperature-dependent magnetization measurement, which suggests a ferromagnetic phase transition occurring at $T_c = 270$ K, in line with the previous report.[24]

The overall electronic structure is illustrated in Fig. 2. We have observed two types of electronic structures in $Fe_{5-x}GeTe_2$ most likely coming from the two different terminations discussed before. Figures 2(a)–2(c)/2(d)–2(f) show the constant energy contour (CEC) in the k_x–k_y plane at E_F, dispersion along the high symmetry $\overline{M}$–$\overline{\Gamma}$–$\overline{M}$ and $\overline{K}$–$\overline{\Gamma}$–$\overline{K}$ directions, and slab calculations along the high symmetry directions for Fe(1)/Fe(5) terminations, respectively. For the Fe(1) termination, we observe triangular petal-like features on the CECs at E_F and characteristic features (denoted as VB_α and VB_β) at higher binding energies. As for the Fe(5) termination, there are a small electron pocket near the $\overline{K}$ point, a distribution of blurred spectral weight near the $\overline{M}$ point and a hexagonal Fermi pocket near the $\overline{\Gamma}$ point, with complex texture structure inside in Fig. 2(d), very similar to the electronic structure of Fe_3GeTe_2.[13] From the high-symmetry dispersions, the characteristic α and β bands correspond to the hole pockets near $\overline{\Gamma}$, while the γ band contributes to the small electron pocket near $\overline{K}$, together with one strong intensity band at the binding energy of 0.5 eV, which may come from the d orbital of excess Fe atoms. The observed characteristic bands could be captured in the slab calculations (Figs. 2(c) and 2(f)), together with other features, indicating the multiband nature of the $Fe_{5-x}GeTe_2$ system.

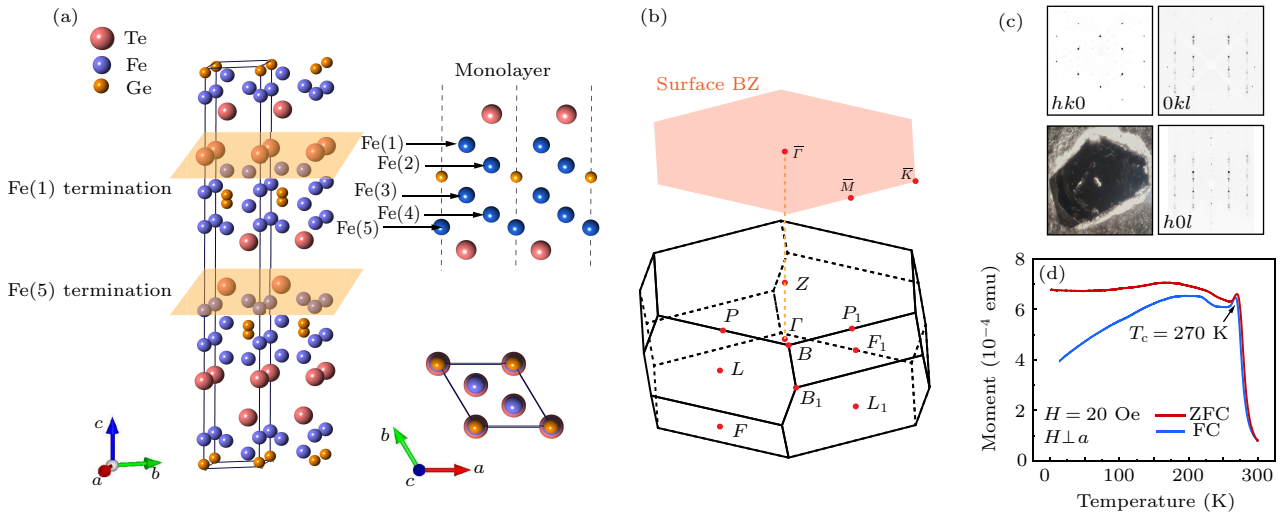


Fig. 1. Basic characterization of $Fe_{5-x}GeTe_2$. (a) Crystal structure of $Fe_{5-x}GeTe_2$. Red, blue, and orange spheres indicate Te, Fe, and Ge atoms, respectively. (b) The Brillouin zone (BZ) of $Fe_{5-x}GeTe_2$. High-symmetry points are labeled. (c) Image of $Fe_{5-x}GeTe_2$ single crystal and XRD patterns along three different crystalline directions. (d) The temperature dependent magnetization of $Fe_{5-x}GeTe_2$. The ferromagnetic transition temperature is marked.

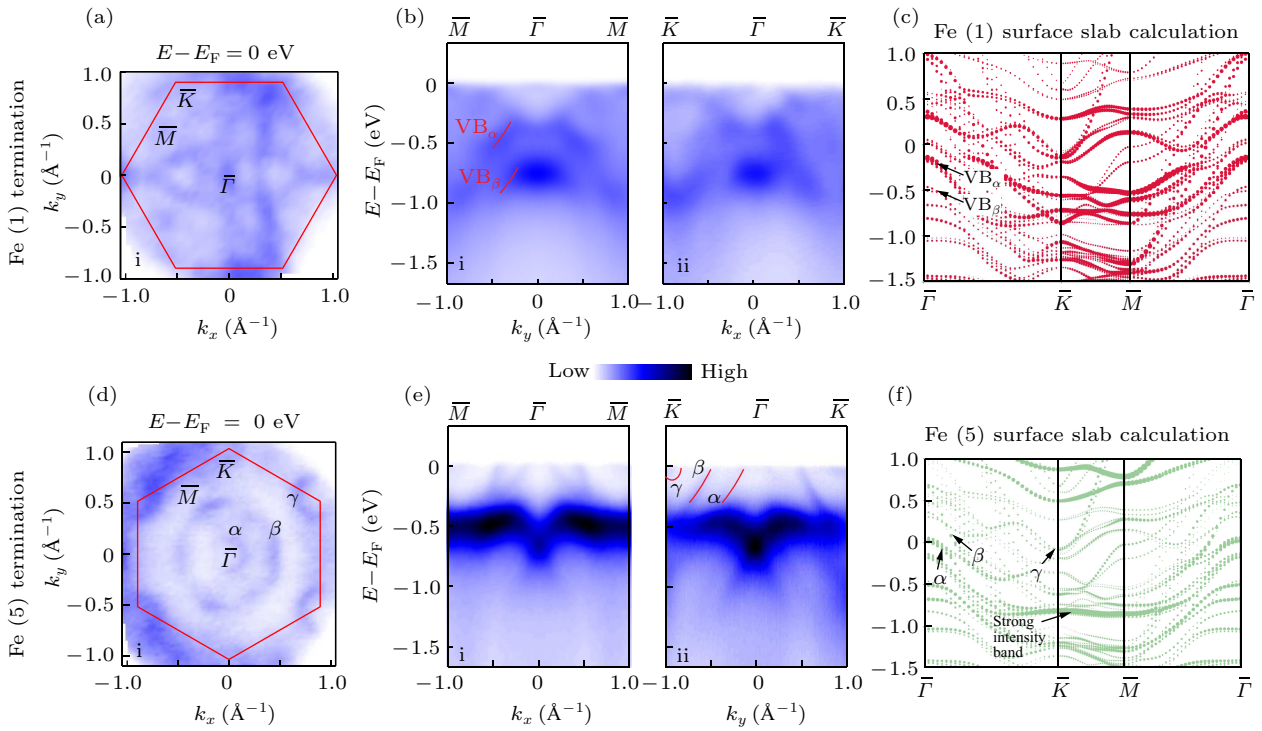


Fig. 2. Overall electronic structure of $Fe_{5-x}GeTe_2$ with two cleaved terminations. (a), (d) Photoemission intensity map of constant energy contours (CECs) in the k_x–k_y plane at E_F of two cleaved terminations, respectively. The asymmetric pattern is due to the photoemission matrix element effect. (b), (e) Band dispersions along high-symmetry $\overline{M}$–$\overline{\Gamma}$–$\overline{M}$ and $\overline{K}$–$\overline{\Gamma}$–$\overline{K}$ of two cleaved terminations, respectively. (c), (f) Slab calculation of Fe_5GeTe_2 in the ferromagnetic state of two cleaved terminations, respectively. The integrated energy window of CECs is ±50 meV. The data were collected using photons with $h\nu = 90$ eV at 12 K.

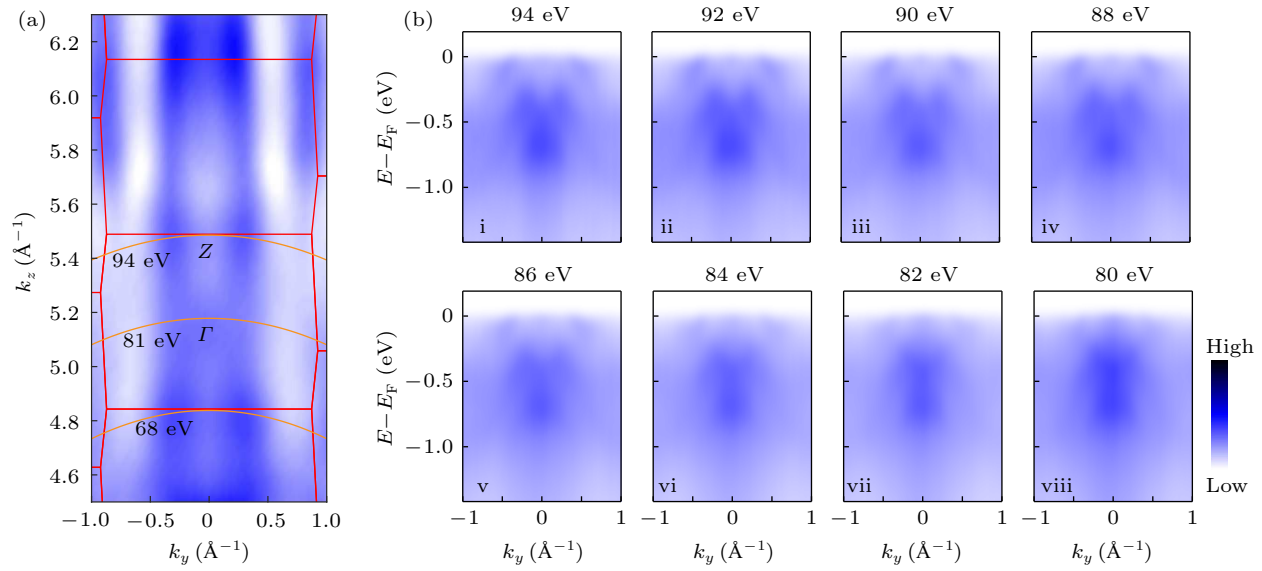


Fig. 3. The k_z evolution of the electronic structure of $Fe_{5-x}GeTe_2$. (a) Photoemission intensity map of the CEC in the k_z–k_y plane at 0.4 eV below E_F. Red line indicates the BZ. The orange line represents the photon energy corresponding to the high symmetry point. (b) Band dispersions along high-symmetry $\overline{M}$–$\overline{\Gamma}$–$\overline{M}$ directions with different photon energy, respectively. The integrated energy window of CECs is ±50 meV. The data were collected at 12 K.

To investigate the evolution of the electronic structure along the k_z direction, photon energy-dependent ARPES experiment was performed on Fe(1) termination with the result shown in Fig. 3. The CEC at 0.4 eV below E_F in the k_y–k_z plane is plotted in Fig. 3(a), where clear periodic patterns are observed with a periodicity of $2\pi/c$ (the BZ is indicated by the red lines with high-symmetry points labeled), allowing us to determine the high symmetry points in the 3D BZ. Figure 3(b) shows the dispersion taken at photon energy from 80 eV to 94 eV along the $\overline{M}$–$\overline{\Gamma}$–$\overline{M}$ direction (which spans half of a BZ). While the energy band near the Fermi surface evolves slightly with the photon energy, the bands located at higher energies show no k_z evolution, which reflects the 2D nature of the $Fe_{5-x}GeTe_2$ compounds.

Finally, we examine the temperature evolution of the electronic bands from the ARPES data on Fe(1) termination. As

shown in the plot of the original data of the ARPES intensity (Fig. 4(a)), we can see clearly that the splitting between the VB_α and VB_β bands becomes smaller as the temperature increases. When the temperature is higher than the T_c (~ 270 K), VB_α and VB_β merge into one energy band (indicated by VB). When the temperature drops back below T_c, VB splits into VB_α and VB_β again, ruling out the band evolution due to simple sample aging. The change of the band splitting is also clearly shown by the side-by-side comparison of stacking plot of momentum distribution curves (MDCs) between the band structures at 12 K and 290 K (Fig. 4(b)), as well as the temperature evolution of the EDCs at $k_y = 0.4$ Å^{-1} (Fig. 4(c)). We extract the peak positions of the VB_α and VB_β, plot their evolution at various temperatures (Fig. 4(d)) and clearly see that the band splitting closes rapidly above T_c.

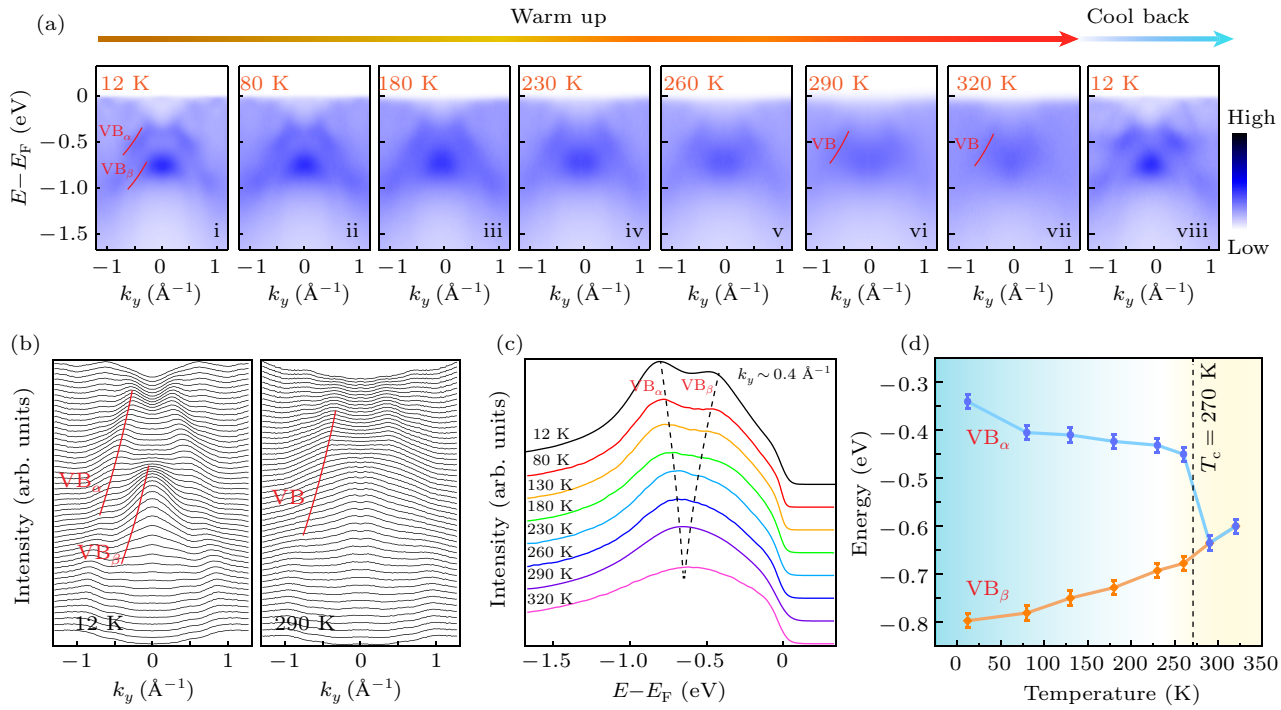


Fig. 4. Temperature evolution of the electronic structure of $Fe_{5-x}GeTe_2$. (a) Band dispersions along high-symmetry $\overline{M}$–$\overline{\Gamma}$–$\overline{M}$ directions at selected temperature. (b) The comparison of stacking plot of momentum distribution curves (MDCs) at 12 K and 290 K. The bands discussed are labeled. (c) The temperature evolution of EDCs at $k_y \sim 0.4$ Å^{-1}. (d) The energy position of VB_α and VB_β bands as functions of temperature. The data were collected using 90 eV photons.

In addition to the change in the splitting between the VB_α and VB_β bands with increasing temperature, other complex evolutions of band structures also occur, such as the disappearing of several features near the Fermi surface (Fig. 4(a)). Although it would be quite difficult to explain the temperature evolution of the band structure of $Fe_{5-x}GeTe_2$ across the ferromagnetic phase transitions, especially given the $\sqrt{3} \times \sqrt{3}$ reconstruction reported[25] which makes the tracing of all the bands difficult, the observed band structure evolution strongly suggests the exchange splitting of VB_α and VB_β in the ferromagnetic phase. Such scenario is showing stark contrast with the band evolution of Fe_3GeTe_2 (and other 2D ferromagnets such as CrI_3 and $Cr_2Ge_2Te_3$)[13,26,27] and consistent with the itinerant Stoner model. We argue the large magnetic moment in $Fe_{5-x}GeTe_2$ (6.659 μ_B/Fe, the largest among the existing 2D ferromagnets[24]) as well as the Fe origin of the band structure observed near E_F may explain the pronounced exchange splitting (~ 400 meV) observed in $Fe_{5-x}GeTe_2$.

3. Conclusion

We have presented systematic investigation of the electronic structure of $Fe_{5-x}GeTe_2$. Our ARPES measurement revealed complete band structure from two different cleaved terminations. In addition, we observed a clear periodic pattern with a periodicity of $2\pi/c$ and exchange splitting of the valence band on the Fe(1) termination. Our results provide important experimental evidence of the electronic structure of $Fe_{5-x}GeTe_2$, and will also help to understand the magnetic origin and interaction between electrons and magnetic order of other two-dimensional ferromagnetic systems.

4. Method

4.1. Crystal growth

High-quality $Fe_{5-x}GeTe_2$ single crystals were grown by using the chemical vapor transport technique via employing iodine as the transport agent. Mixtures of high purity elements including Fe, Ge, and Te with ratio of 6 : 1 : 2 were mixed

and sealed in an evacuated quartz tube and slowly heated up to 700 °C in a tubular furnace. After stayed at the temperature for 7 days, the assembly was slowly cooled down to room temperature.

4.2. Angle-resolved photoemission spectroscopy

The ARPES measurements were performed at BL03U station at Shanghai Synchrotron Radiation Facility (SSRF), China, beam line I05 of the Diamond Light Source (DLS), UK. The $Fe_{5-x}GeTe_2$ single crystals were first elaborately selected and well prepared in air. Then they were cleaved *in situ* along the (001) surface without spoiling, and measured at a 12 K sample temperature in ultrahigh vacuum with a base pressure of lower than 7×10^{-11} Torr. Data were recorded by a VG Scienta DA30 analyzer. The angle resolution was 0.2° and the overall energy resolutions were better than 15 meV.

4.3. Density functional theory calculations

DFT calculations were performed using the generalized gradient approximation for the exchange correlation potential with a plane-wave basis and the projector augmented wave method as implemented in the Vienna *ab initio* simulation package (VASP).[28–30] The energy cut-off for the plane wave was set to 700 eV for structural relaxation and 500 eV for electronic structure calculations, and the k-point sampling was $15 \times 15 \times 1$. The slab is composed of two sub-layers, and the vacuum layer is larger than 15 Å. The Fe1 atoms are above the Ge atoms in each sub-layer. The structures were fully relaxed until the residual force per atom was less than 0.001 eV/Å. In structural relaxation calculations, dispersion correction was considered in the optB86b functional for the exchange potential.[31] DFT+U method[32] was used to better describe the strong correlation system in structural relaxation and electronic structures. $U = 1$ eV was chosen in our calculations, and the lattice parameter $a = b = 4.04$ Å. Spin–orbit coupling effect and ferromagnetism were considered in electronic structure calculations.

Acknowledgments

This research used BL03U of Shanghai Synchrotron Radiation Facility and I05 of the Diamond Light Source. We also acknowledge the Analytical Instrumentation Center of ShanghaiTech University for x-ray diffraction and MPMS measurements. Z. K. Liu acknowledges the National Key R&D Program of China (Grant No. 2017YFA0305400).

References

[1] Huang B, Clark G, Navarro-Moratalla E, Klein D R, Cheng R, Seyler K L, Zhong D, Schmidgall E, McGuire M A, Cobden D H, Yao W, Xiao D, Jarillo-Herrero P and Xu X 2017 *Nature* **546** 270

[2] Gong C, Li L, Li Z, Ji H, Stern A, Xia Y, Cao T, Bao W, Wang C, Wang Y, Qiu Z Q, Cava R J, Louie S G, Xia J and Zhang X 2017 *Nature* **546** 265

[3] Liu B, Zou Y, Zhang L, Zhou S, Wang Z, Wang W, Qu Z and Zhang Y 2016 *Sci. Rep.* **6** 33873

[4] Lin G T, Zhuang H L, Luo X, Liu B J, Chen F C, Yan J, Sun Y, Zhou J, Lu W J, Tong P, Sheng Z G, Qu Z, Song W H, Zhu X B and Sun Y P 2017 *Phys. Rev. B* **95** 245212

[5] Jiang S, Shan J and Mak K F 2018 *Nat. Mater.* **17** 406

[6] Jiang S, Li L, Wang Z, Mak K F and Shan J 2018 *Nat. Nanotechnol.* **13** 549

[7] Mermin N D and Wagner H 1966 *Phys. Rev. Lett.* **17** 1133

[8] Lin M W, Zhuang H L, Yan J, Ward T Z, Puretzky A A, Rouleau C M, Gai Z, Liang L, Meunier V, Sumpter B G, Ganesh P, Kent P R C, Geohegan D B, Mandrus D G and Xiao K 2016 *J. Mater. Chem. C* **4** 315

[9] Bonilla M, Kolekar S, Ma Y, Diaz H C, Kalappattil V, Das R, Eggers T, Gutierrez H R, Phan M H and Batzill M 2018 *Nat. Nanotechnol.* **13** 289

[10] O'Hara D J, Zhu T, Trout A H, Ahmed A S, Luo Y K, Lee C H, Brener M R, Rajan S, Gupta J A, McComb D W and Kawakami R K 2018 *Nano Lett.* **18** 3125

[11] Deng Y, Yu Y, Song Y, Zhang J, Wang N Z, Sun Z, Yi Y, Wu Y Z, Wu S, Zhu J, Wang J, Chen X H and Zhang Y 2018 *Nature* **563** 94

[12] Fei Z, Huang B, Malinowski P, Wang W, Song T, Sanchez J, Yao W, Xiao D, Zhu X, May A F, Wu W, Cobden D H, Chu J H and Xu X 2018 *Nat. Mater.* **17** 778

[13] Xu X, Li Y W, Duan S R, Zhang S L, Chen Y J, Kang L, Liang A J, Chen C, Xia W, Xu Y, Malinowski P, Xu X D, Chu J H, Li G, Guo Y F, Liu Z K, Yang L X and Chen Y L 2020 *Phys. Rev. B* **101** 201104

[14] Chen B, Yang J, Wang H, Imai M, Ohta H, Michioka C, Yoshimura K and Fang M 2013 *J. Phys. Soc. Jpn.* **82** 124711

[15] Verchenko V Y, Tsirlin A A, Sobolev A V, Presniakov I A and Shevelkov A V 2015 *Inorg. Chem.* **54** 8598

[16] Stahl J, Shlaen E and Johrendt D 2018 *Zeitschrift für Anorg. und Allg. Chemie* **644** 1923 (in France)

[17] May A F, Ovchinnikov D, Zheng Q, Hermann R, Calder S, Huang B, Fei Z, Liu Y, Xu X and McGuire M A 2019 *ACS Nano* **13** 4436

[18] Kim K, Seo J, Lee E, Ko K T, Kim B S, Jang B G, Ok J M, Lee J, Jo Y J, Kang W, Shim J H, Kim C, Yeom H W, Il Min B, Yang B J and Kim J S 2018 *Nat. Mater.* **17** 794

[19] You Y, Gong Y, Li H, Li Z, Zhu M, Tang J, Liu E, Yao Y, Xu G, Xu F and Wang W 2019 *Phys. Rev. B* **100** 134441

[20] Zhang Y, Lu H, Zhu X, Tan S, Feng W, Liu Q, Zhang W, Chen Q, Liu Y, Luo X, Xie D, Luo L, Zhang Z and Lai X 2018 *Sci. Adv.* **4** eaao679

[21] Ding B, Li Z, Xu G, Li H, Hou Z, Liu E, Xi X, Xu F, Yao Y and Wang W 2020 *Nano Lett.* **20** 868

[22] Zhuang H L, Kent P R C and Hennig R G 2016 *Phys. Rev. B* **93** 134407

[23] May A F, Bridges C A and McGuire M A 2019 *Phys. Rev. Mater.* **3** 104401

[24] Li Z, Xia W, Su H, Yu Z, Fu Y, Chen L, Wang X, Yu N, Zou Z and Guo Y 2020 *Sci. Rep.* **10** 15345

[25] Wu X, Lei L, Yin Q, Zhao N N, Li M, Wang Z, Liu Q, Song W, Ma H, Ding P, Cheng Z, Liu K, Lei H and Wang S 2021 *Phys. Rev. B* **104** 165101

[26] Watson M D, Marković I, Mazzola F, Rajan A, Morales E A, Burn D M, Hesjedal T, van der Laan G, Mukherjee S, Kim T K, Bigi C, Vobornik I, Ciomaga Hatnean M, Balakrishnan G and King P D C 2020 *Phys. Rev. B* **101** 205125

[27] Zhang Y, Holder T, Ishizuka H, de Juan F, Nagaosa N, Felser C and Yan B 2019 *Nat. Commun.* **10** 3783

[28] Blöchl P E, Jepsen O and Andersen O K 1994 *Phys. Rev. B* **49** 16223

[29] Kresse G and Joubert D 1999 *Phys. Rev. B* **59** 1758

[30] Kresse G and Furthmüller J 1996 *Phys. Rev. B* **54** 11169

[31] Klimeš J, Bowler D R and Michaelides A 2011 *Phys. Rev. B* **83** 195131

[32] Anisimov V I, Aryasetiawan F and Lichtenstein A I 1997 *J. Phys. Condens. Matter* **9** 767